Determination of Nitrogen in Sand Using Laser-Induced Breakdown Spectroscopy

RONNY D. HARRIS, DAVID A. CREMERS,* MICHAEL H. EBINGER, and BRIAN K. BLUHM

Group NMT-15 (R.D.H., B.K.B.), Group C-ADI (D.A.C.), and Group EES-2 (M.H.E.), Los Alamos National Laboratory, Los Alamos, New Mexico 87545

The use of laser-induced breakdown spectroscopy (LIBS) to detect a variety of elements in soils has been demonstrated and instruments have been developed to facilitate these measurements. The ability to determine nitrogen in soil is also important for applications ranging from precision farming to space exploration. For terrestrial use, the ideal situation is for measurements to be conducted in the ambient air, thereby simplifying equipment requirements and speeding the analysis. The high concentration of nitrogen in air, however, is a complicating factor for soil nitrogen measurements. Here we present the results of a study of LIBS detection of nitrogen in sand at atmospheric and reduced pressures to evaluate the method for future applications. Results presented include a survey of the nitrogen spectrum to determine strong N emission lines and determination of measurement precision and a detection limit for N in sand (0.8% by weight). Our findings are significantly different from those of a similar study recently published regarding the detection of nitrogen in soil.

Index Headings: **Laser-induced breakdown spectroscopy; LIBS; Nitrogen; Sand; Soil.**

INTRODUCTION

In recent years, laser-induced breakdown spectroscopy (LIBS) has been studied and developed to determine a variety of elements in soils. Applications include general soil analysis, the screening of soils for toxic metals for environmental monitoring programs,[1–6] and monitoring carbon in soil for use in terrestrial carbon sequestration programs[7–10] aimed at mitigating greenhouse gases. LIBS has been shown to be useful for these applications and some field deployable instruments have been developed.[11,12] There is also interest in LIBS for determining elements, including nitrogen, in geological samples on planetary surfaces.[13–15] Nitrogen detection has also been used to identify energetic materials[16] and organic compounds.[17] The detection of N along with other elements including P and K are of interest to precision farming implementation.[18,19] LIBS may have application in this area because of its field-deployable capabilities. However, nitrogen, being a major (80%) constituent of air, represents a challenge, unlike most other elements, when detection must be conducted at atmospheric pressure. Emissions from neutral and once-ionized nitrogen species are readily observed when the laser plasma is formed in air[20] or on a solid surface in air, and these can predominate over nitrogen emission originating from a solid target. In addition, nitrogen has few strong emission lines that can be observed after the first few microseconds following plasma formation when the strong background continuum light has decayed. These difficulties are related to the high energy of the upper levels of the nitrogen lines, typically >11 eV in the visible and near-ultraviolet (UV) spectral regions, and the high ionization potential of N(I) (14.53 eV). Stronger N(I) emissions occur in the vacuum ultraviolet region between 119.96–120.07 nm and 149.26–149.47 nm, but these emissions are not accessible for many applications.

Here we present a study of the characteristics of the detection of nitrogen in sand at and below atmospheric pressure. Sand was used as a surrogate for soil to minimize the number of spectral interferences in analyzing the nitrogen spectrum. We also investigate a recent claim of the ability to detect nitrogen in soil in an air environment[9,10] and present our findings on this topic.

EXPERIMENTAL

Apparatus. A 150 mm diameter × 60 mm high evacuable chamber was constructed to allow analysis of samples at reduced pressures. The chamber contained a 50 mm diameter fused-silica window to allow transmittance of the laser beam as well as ultraviolet light emitted from the laser plasma. A rotatable sample stage was used to position each sample under the window for subsequent analysis. The stage allowed sequential analysis of eight different samples under similar conditions in the sealed chamber. It also allowed movement of the sample during analysis to prevent excessive ablation in one area by the repetitive laser pulses and to promote random sampling of the surface. A Tribodyne vacuum pump (Danielson) was used to create an evacuated environment with pressures as low as 0.04 torr. A micrometer valve on the housing of the chamber made it possible to achieve stable intermediate pressures between 590 torr (normal atmospheric pressure at Los Alamos, NM) and 0.04 torr by flowing gas through the chamber while pumping. The chamber pressure was measured using a model 275 Convectron Gauge (Granville-Phillips).

Laser pulses from a Q-switched Nd : YAG laser (Quanta-Ray, Model DCR-11, Gaussian-like spatial profile, 1064 nm wavelength, 10 Hz, 10 ns duration) were focused vertically onto the sample surface using a lens with a 100 mm focal length. The lens was attached to a stage outside the chamber making it easy to adjust the lens-to-sample distance (LTSD). Laser energies of 18–150 mJ/pulse were used to produce a reproducible laser spark, depending on experimental conditions (e.g., LTSD, air pressure). Laser power was monitored using an Astral AD 30 meter with an AC detector head (Scientech).

The emitted light was collected at a distance of 5 cm

Received 2 February 2004; accepted 24 March 2004.
* Author to whom correspondence should be sent.

0003-7028/04/5807-0770$2.00/0

TABLE I. Wavelengths and relative intensities of nitrogen emissions in a LIBS plasma.

Wavelength (nm) and species	Rel. intensity Al target, I_{Rel} (Al)	Rel. intensity in air plasma, I_{Rel} (air)	I_{Rel} (Al)/I_{Rel} (air)
343.72 (II)	0.041	0.042	0.98
391.90 (II)	0.045	0.037	1.22
395.59 (II)	. . .	0.022	. . .
399.50 (II)	0.439	0.289	1.52
403.51/404.13/404.35 (II)	0.098	0.069	1.42
444.70 (II)	0.118	0.086	1.37
460.15 (II)	0.065	0.073	0.89
460.72 (II)	0.065	0.059	1.10
461.39 (II)	0.057	0.039	1.46
462.14 (II)	0.094	0.061	1.54
463.05 (II)	0.264	0.208	1.27
464.31 (II)	0.073	0.064	1.14
480.33 (II)	. . .	0.034	. . .
499.44–502.57 (II)[a]	0.504	0.347	1.45
504.51 (II)	. . .	0.042	. . .
566.66 (II)	. . .	0.051	. . .
567.60/567.96 (II)	0.126	0.144	0.88
742.36 (I)	0.110	0.093	1.18
744.23 (I)	0.382	0.435	0.88
746.83 (I)	1	1	1

[a] Unresolved grouping of lines including: 499.44, 500.15, 500.27, 500.52, 500.73, 501.06, 501.64, and 502.57 nm.

by a fused-silica fiber-optic cable (C-Technologies, Inc.) pointed at the plasma but positioned outside the experimental chamber. The fiber-optic cable was fixed at an angle of 75 degrees with respect to the sample surface. The light was transported a distance of 2 m through the fiber-optic cable to the entrance slit (50 μm width) of a 0.5 m focal length spectrograph (Chromex Imaging Spectrograph, Model 500IS). A 1200 lines/mm grating was used to resolve emitted light in the 500 and 740 nm regions of the spectrum. The detector was a gated intensified charge-coupled device (CCD) (Oriel, InstaSpec V). A digital delay/pulse generator (Stanford Research Systems, Inc., Model DG535) was used to control the exact time that data were recorded. For most experiments the delay time (t_d) was 0 ns, referring to the time after plasma formation at which the intensifier on the detector was turned on. The box width (t_b) was 20 μs, referring to the length of time over which the intensifier was gated on.

Each measurement involved averaging the spectra from 100 laser shots to produce a single spectrum. Spectra were analyzed using an in-house computer program (LabView®) that integrates the area under a selected peak or determines the peak height. When constructing calibration curves, five replicate measurements were made using each nitrogen standard, and the data from these were averaged to produce a single nitrogen signal at a known nitrogen concentration.

An integrated echelle spectrograph system (Model ESA 3000, LLA GmbH) was used for simultaneous determination of the relative intensities of nitrogen emission lines in the UV/visible region (Table I). This system has a spectral range from 200 to 780 nm, but there were several gaps in the near-infrared region of the spectrum preventing the detection of some nitrogen lines in this region. The spectral response of the echelle system was calibrated using NIST traceable deuterium–tungsten calibration lamps, allowing correction for total detection system efficiency over the entire spectral range monitored. A laser energy of 150 mJ/pulse was used to produce the spark in air while 60 mJ/pulse was used on the Al target. The values of t_d and t_b used to record the LIBS nitrogen spectra were 350 ns and 10 μs, respectively.

Sample Preparation. Sea sand was used here instead of soil to minimize spectral interferences from minor and trace elements. The results obtained here should apply to the detection of nitrogen in soil. Washed sea sand (Fisher) was spiked with various quantities of Super Turf Builder® (Scotts) to produce 7 standards ranging from 0.33 to 6.04% N by weight. Super Turf Builder® (36% total N) is derived from several sources of nitrogen, including ammoniacal nitrogen, urea, methylenediurea, and dimethylenetriurea. Spectrographic X-ray Mix Powder (Chemplex Industries) was used in each sample as a grinding and briquetting additive. Samples of sea sand and the briquetting additive were analyzed by dry combustion (VarioMax CN Macro Elemental Analyzer, Elementar Analysensysteme GmbH) to confirm the absence of nitrogen (limit of detection = 100 ppm N) in those substances prior to spiking. Samples containing precisely measured masses of turf builder, sea sand, and briquetting additive were homogenized and mixed for approximately 5 min using a mortar and pestle. Three grams of each sample was placed into a 30 mm diameter aluminum Spec Cap (SPEXCertiPrep) and pressed using 20 tons of force (Carver Press, Model M) for 3 min. This process produced samples with flat, packed surfaces and minimized variations in signal due to sample spatial heterogeneity. Titanium metal slugs (Alfa Products) and Al plates (machining stock) were used as a source of Ti spectra and as a low-spectral-density metal for surface studies, respectively.

RESULTS AND DISCUSSION

Nitrogen Spectrum. Nitrogen emission lines from a laser-induced plasma were recorded using the ESA 3000 echelle spectrograph system, relative line intensities were computed, and the results are listed in Table I. Data extend from 343 to 746 nm and are corrected for the spectral response of the ESA 3000 system. Measurements were carried out both with the laser plasma generated directly in air (150 mJ/pulse) and with the plasma formed on an Al metal surface (60 mJ/pulse). Aluminum was used as the target instead of soil or sand because Al exhibits a low density of emission lines, reducing the chance of interference with nitrogen lines. Emission lines for each target are listed relative to the strongest line observed from that target, which was N(I) at 746.83 nm in both cases. The majority of observed lines originate from once-ionized nitrogen, but the strongest observed lines are due to N(I) for the time settings used here (t_d = 350 ns, t_b = 10 μs). The right column of Table I compares the relative strength of each line for the two targets. In the majority of cases, emission from N(II) appears enhanced for the plasma generated on a target compared to the air plasma, especially when considering the fact that less energy was used to create the plasma on Al metal.

Effect of Pressure. Figure 1 shows the strong emissions from N(II) centered around 501 nm using the laser plasma generated on an Al metal plate in air. Measurements were carried out at the ambient pressure of 590

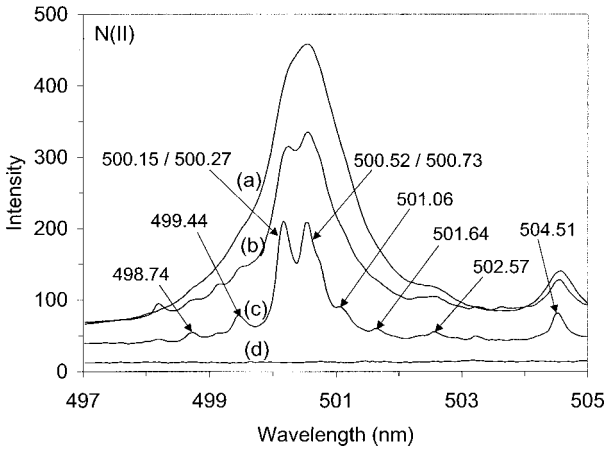

FIG. 1. LIBS spectra of nitrogen from an Al metal target maintained in air at (***a***) 590, (***b***) 100, (***c***) 10, and (***d***) 0.04 torr. For display here, the counts for (a), (b), and (c) were divided by 1000 and for (d) the factor was 500.

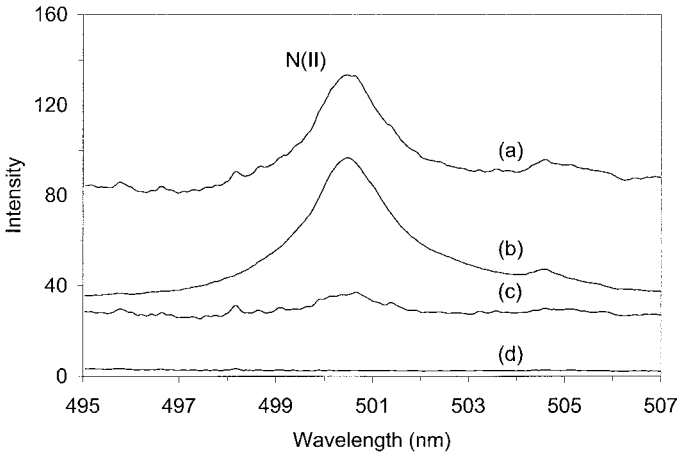

FIG. 2. LIBS spectra of nitrogen from an Al metal target in air at 590 torr using a delay (t_d) of (***a***) 0, (***b***) 200, (***c***) 300, and (***d***) 500 ns.

torr (Los Alamos atmospheric pressure) and at reduced pressures of 100, 10, and 0.04 torr. Spectra were acquired by averaging 100 shots and using t_d = 0 μs (t_b = 20 μs). The N(II) peaks shown in Fig. 1 completely disappear using a 500 ns or greater delay time. In this spectral region there is a high density of N(II) lines that are not resolved at 590 torr. As the pressure is reduced, the individual lines become more resolved and the peak wavelengths can definitely be attributed to N(II). Even at a pressure of 10 torr (Fig. 1c) there is a significant signal from N(II) due to the residual atmosphere. At 0.04 torr (Fig. 1d), however, no N(II) emissions are observed. For the experimental conditions used here, the disappearance of nitrogen emissions at 0.04 torr is reasonable. The peak intensity shown in Fig. 1c is 460 000 counts, and if the N(II) signal is directly proportional to its concentration in air, then at the reduced pressure the N(II) signal should be 460 000/(590/0.04) = 31 counts, which is very close to the background signal shown in Fig. 1d where no peaks are present. These results suggest that N(II) signals recorded from solid samples analyzed at a pressure of 0.04 torr or below can be attributed to nitrogen arising from the solid rather than from the ambient air.

Effect of Delay Time. As noted above, the N(II) lines decrease in intensity strongly as the delay time is increased. This is shown in Fig. 2 for a laser plasma formed on Al metal in air at 590 torr. As t_d is increased from 0 to 300 ns, the unresolved emissions decrease significantly and at a 500 ns delay they are completely absent. Note that as the delay is increased the individual lines did not become apparent, indicating that reduced pressure (Fig. 1) is the main parameter that determines resolution of the separate N(II) lines.

Detection of Nitrogen in Sand. As noted above, the ideal situation for terrestrial applications is for the detection of nitrogen in soil to be carried out in ambient air, and recent work by others has described this capability using LIBS.[9,10] After significant effort, however, we were unable to reproduce the N(II) emission spectrum in the 501 nm region shown in the previously published work. In fact, except for the line labeled 501.6 nm, the emission wavelengths listed on the spectrum shown in this work (e.g., 498.2, 498.9, 499.9, 500.6, and 503.0 nm) do not coincide with compilations of N(I) or N(II) emission line wavelengths.[21,22] Our studies indicate that the emission lines shown in Refs. 9 and 10 are actually due to Ti(I) lines, which are usually observed in most soils and which were present in the sea sand. Figure 3 illustrates this fact, showing LIBS spectra of sea sand containing 2.2% N obtained in air (590 torr) using LTSD values of (a) 100, (b) 97, and (c) 94 mm. For these measurements the laser energy was set at 22 mJ to reduce air nitrogen excitation. As noted above in the Al metal experiments, the delay must be set to a very early time (e.g., 0 μs) to observe the N(II) lines. The focal length of the lens was 100 mm so that the focal point of the laser excitation in Fig. 3a was exactly on the surface of the sample. Visual inspection of the laser plasma formed on a sample showed that at an LTSD of 100 mm, the bottom of the plasma was indeed incident on the sample surface and a damage spot of minimal diameter was formed. The excitation of N(II) is observed as indicated in Fig. 3a by the broad unresolved emission peak around 501 nm, similar to that shown in Fig. 1a for Al at 590 torr. In Fig. 3b the focal point is 3 mm into the sample (LTSD = 97 mm), and in Fig. 3c the focal point is 6 mm into the sample (LTSD = 94 mm). As the LTSD is decreased in Figs. 3b and 3c,

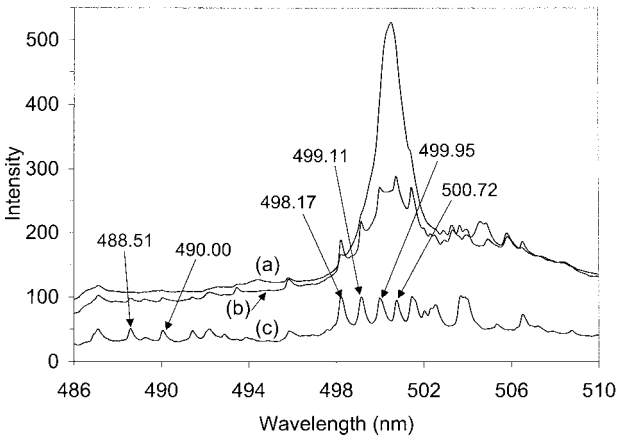

FIG. 3. LIBS spectra of sea sand containing 2.2% nitrogen using LTSD values of (***a***) 100, (***b***) 97, and (***c***) 94 mm.

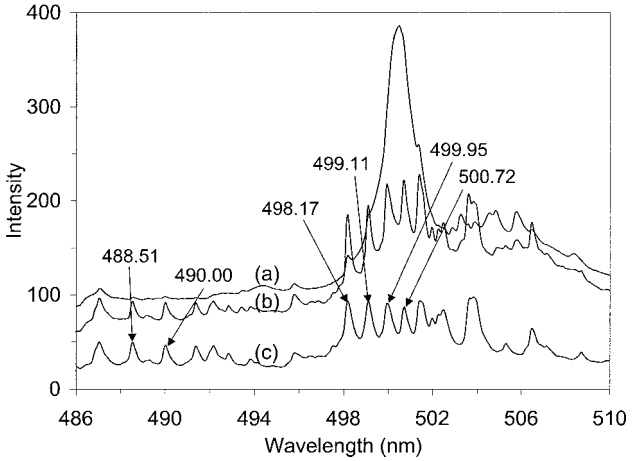

FIG. 4. LIBS spectra of sea sand containing 0.0% nitrogen using LTSD values of (***a***) 100, (***b***) 97, and (***c***) 94 mm.

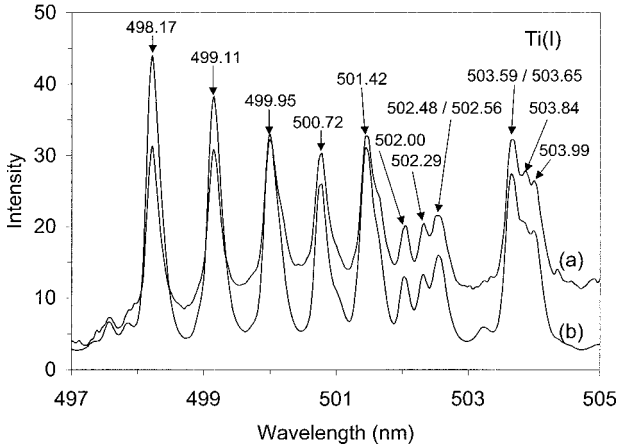

FIG. 5. LIBS spectra of (***a***) Ti metal at 0.04 torr and (***b***) sea sand containing 2.2% nitrogen in air at 590 torr.

the energy density of the laser pulse on the sample surface is also decreased, producing significant changes in the spectra. Thus, different emission peaks become apparent when the excitation above the sample surface is reduced by adjusting the LTSD. It appears that much of the emission from nitrogen in air above the sample (501 nm) is eliminated from the spectra by making the proper LTSD adjustment. In fact, decreasing the LTSD to 90 mm reduced the energy density incident on the sample surface to the extent that no plasma was produced when using a laser pulse energy of 22 mJ (data not shown). Since the sample used in Fig. 3 contains 2.2% N, N(II) peaks should be visible if they are sufficiently excited in the laser plasma. Analysis of Figs. 3b and 3c indicate that when lower energy densities are used in the 500 nm region, the peaks that appear correspond to strong Ti(I) lines of emission as verified in wavelength compilations. Comparison of the spectrum of Fig. 3c from 497 to 505 nm, which we attribute to Ti(I), appears identical to the spectrum attributed to N(II) in the previous work.[9,10] Peaks that appear at 488.51 and 490.00 nm in Fig. 3c are also characteristic of Ti(I).

Spectra contained in Fig. 4, obtained using 18 mJ/pulse, further support the idea that the emission lines in Fig. 3 are due to Ti(I) and not N(II). Here LIBS spectra of sea sand containing 0.0% N (as verified by dry combustion analysis) in air at 590 torr using LTSD values of (a) 100, (b) 97, and (c) 94 mm are shown for comparison with Fig. 3. The changes in both sets of spectra as a function of LTSD are essentially identical. The spectra in Fig. 4 with no added N are essentially the same as the spectra in Fig. 3 with 2.2% added N; thus, the added nitrogen was not observed. The spectra in Figs. 3 and 4 are similar because the peaks are due to Ti(I), which is present in the sea sand.

Figure 5 contains additional data confirming that the spectra presented in Figs. 3b and 3c and 4b and 4c display emission lines due to Ti(I) rather than N(II). Figure 5 presents LIBS spectra of (a) high purity Ti metal in 0.04 torr air and (b) sea sand containing 2.2% nitrogen in air at 590 torr. The spectrum of Ti was obtained using a pulse energy of 60 mJ and an LTSD of 97 mm in order to form an analytically useful spark at the lower pressure. As demonstrated above (Fig. 1), nitrogen from air was not observed from the laser plasma formed on a metal surface at a pressure of 0.04 torr; therefore, all lines observed from the pure Ti sample in Fig. 5a were unquestionably due to Ti. The measurements using sea sand (Fig. 5b) were conducted with an LTSD of 97 mm, which according to Fig. 3b should produce a low enough plasma density to exclude most of the atmospheric nitrogen from the measurements. The laser pulse energy was also reduced to 18 mJ to duplicate the energy used to obtain the spectra shown in Figs. 3 and 4, which generated plasmas that produced emission lines characteristic of the sample surface rather than the surrounding atmosphere. The reduced laser pulse energy is also similar to that used in the previously published work on detection of nitrogen in soil.[9,10] Comparison of the Ti spectrum taken in an environment with negligible atmospheric nitrogen (Fig. 5a) to that recorded from sea sand containing 2.2% N (Fig. 5b) shows that the emission features are identical. This proves that the observed peaks in the 501 nm region for the N containing sea sand at atmospheric pressure are solely due to Ti.

Nitrogen Calibration Curve. Investigation of N(II) lines between 499.44 and 502.57 nm showed that it was not possible to use these lines to construct a calibration curve for nitrogen in sea sand at atmospheric and reduced pressures. The emissions observed at atmospheric pressure and at the higher pulse energy densities used here could always be related to nitrogen from air. In contrast, emissions observed at atmospheric pressure and low pulse energy densities were always characteristic of Ti(I) lines from the sea sand. At reduced pressures, the nitrogen lines due to N(II) were not observed from a sea sand sample containing up to 6% N. Attempts to observe the N(II) lines from the sea sand samples at 0.04 torr using a variety of different delay times and LTSD values were not successful.

It was possible, however, to generate a useful nitrogen calibration curve using N(I) lines in the spectral region 741–749 nm if the samples were analyzed at a reduced pressure of 0.04 torr and at a laser pulse energy of 60 mJ. The intensities of these lines recorded from sea sand samples containing 6.0, 1.5, and 0.3% nitrogen are shown in Fig. 6. For the three N(I) lines monitored here (742.36, 744.23, and 746.83 nm), it is clear that the emission lines

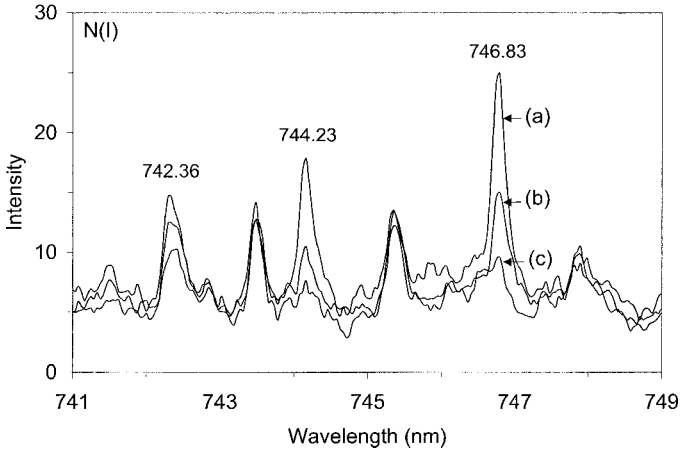

FIG. 6. LIBS spectra at 0.04 torr air of sea sand containing nitrogen at concentrations of (***a***) 6.0%, (***b***) 1.5%, and (***c***) 0.3% by weight.

decrease in intensity along with decreased nitrogen concentration in the sea sand samples.

A calibration curve prepared using nitrogen spiked sea sand samples and the N(I) 746.83 nm peak intensities is shown in Fig. 7. The ambient pressure was 0.04 torr and the pulse energy was 60 mJ. The data points below 1% N have high relative standard deviations (RSD). The percent RSD values obtained here for five replicate measurements (each measurement the average of 100 shots) at each concentration are: 46.6% RSD for 0.33% N, 25.4% RSD for 0.59% N, 47.2% RSD for 0.83% N, 11.1% RSD for 1.48% N, 13.7% RSD for 2.16% N, 7.6% RSD for 2.9% N, and 4.8% RSD for 6.0% N. We believe the high % RSD values at the lower nitrogen concentrations are due to sample heterogeneity, low N(I) signal below 1% N, and the limited number of shots (100) used for each measurement. A limit of detection was computed from the calibration data using the typical formula of $3\sigma/m$, where σ is the standard deviation of a measurement corresponding to an intermediate nitrogen concentration and m is the linear slope of the calibration line. The limit of detection obtained using this method was 0.8% N when applying the standard deviation of the 1.48% N sample. A close inspection of Fig. 7 reveals that the slope of the calibration curve (response) begins to decrease after the 0.83% N sample, indicating the limit of detection.

We attempted to make a calibration curve using the same nitrogen containing samples at 742.36, 744.23, and 746.83 nm at atmospheric pressure (590 torr) rather than 0.040 torr. Here again, to exclude or at least minimize the contribution of atmospheric nitrogen to the N(I) signals, measurements were conducted using 20 mJ/pulse, LTSD = 97 mm, and t_d = 500 ns. The values of pulse energy and LTSD were used to reproduce the experimental conditions specified in the previous study of nitrogen in soil detection[9,10] and to accentuate the nitrogen signal from the soil rather than ambient air. Recall that the N(I) peak intensities decreased with decreasing nitrogen concentration when the data were acquired at 0.040 torr (Fig. 6). Figure 8 shows LIBS spectra obtained from two sea sand samples having nitrogen concentrations that differ by a factor of 60 (0.1 and 6.0% N). The spectra, taken in ambient air (590 torr) using a low plasma energy density, do not show, however, a change in the N(I) peak

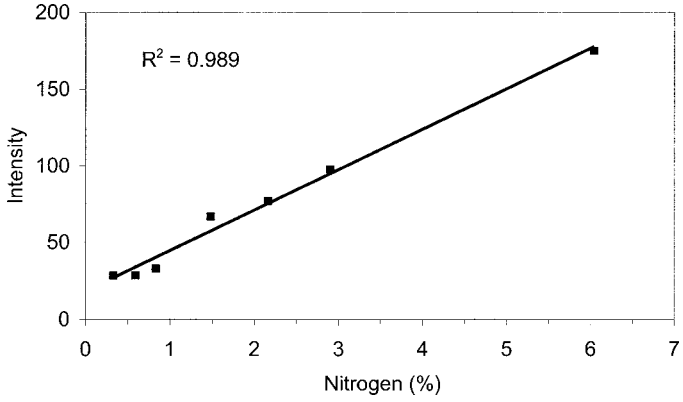

FIG. 7. Nitrogen calibration curve for spiked sea sand samples using N(I) 746.83 nm peak intensities.

intensities between the two samples. This indicates that the constant supply of nitrogen in air is the predominate source of the observed N(I) signal when data are acquired at atmospheric pressure.

CONCLUSION

Using LIBS, it is possible to monitor nitrogen in sand (or soil) if the sample is maintained at reduced pressure. For the conditions of this study, a pressure below 0.04 torr air appears adequate. The best analytical lines in terms of signal strength were the N(I) lines at 746.83 and 744.23 nm. The emission lines due to N(II) centered around 501 nm could not be related to the nitrogen content of the solid sample and always appeared to be due to the surrounding air. This was the case for the different values of LTSD, laser pulse energy, and delay times used here. There are also many Ti(I) lines that interfere with the N(II) lines in the 501 nm region. At reduced pressure, the N(II) lines disappeared and were not observed at the highest nitrogen concentration in sea sand used here (6%). The use of LIBS for the detection of nitrogen in soil will require the development of a sample chamber to exclude nitrogen from air. It may be possible to perform the analysis at slightly higher air pressures (0.1 torr) than used here or at atmospheric pressure in a purge gas with-

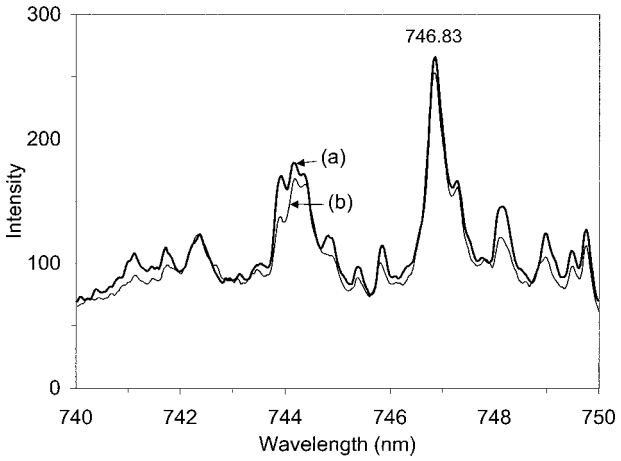

FIG. 8. LIBS spectra of sea sand containing (***a***) 0.1% nitrogen and (***b***) 6.0% nitrogen at 590 torr using an energy of 20 mJ and LTSD of 97 mm.

out nitrogen, but this needs to be investigated. The use of LIBS for the detection of nitrogen in geological samples on Mars (7 torr CO_2) and other bodies with low pressure (e.g., Moon, asteroids) would appear feasible. In addition, in these environments it may be possible to monitor the stronger N(I) emissions in the vacuum ultraviolet spectral region.

ACKNOWLEDGMENTS

This work was partially funded by the Nuclear Materials Technology (Group NMT-15) and Chemistry (Group C-ADI) Divisions at Los Alamos National Laboratory. The authors wish to thank Zane Arp (Group NMT-15) for writing and supporting the data analysis software and Clifton Meyer (Group EES-2) for performing dry combustion analysis of samples. In addition, the authors wish to acknowledge that this work has built upon current efforts at Los Alamos National Laboratory, funded by the Department of Energy's Office of Science and the National Energy Technology Laboratory, in the area of terrestrial carbon sequestration. Los Alamos National Laboratory is operated by the University of California for the U.S. Department of Energy.

1. F. Capitelli, F. Colao, M. R. Provenzano, R. Fantoni, G. Brunetti, and N. Senesi, Geoderma **106,** 45 (2002).
2. M. F. Bustamante, C. A. Rinaldi, and J. C. Ferrero, Spectrochim. Acta, Part B **57,** 303 (2002).
3. A. Ciucci, V. Palleschi, S. Rastelli, R. Barbini, F. Colao, R. Fantoni, A. Palucci, S. Ribezzo, and H. J. L. van der Steen, Appl. Phys. B **63,** 185 (1996).
4. G. Theriault, P. A. Mosier-Boss, and S. H. Lieberman, Proc. SPIE-Int. Soc. Opt. Eng. **3535,** 141 (1998).
5. J. M. Vadillo, K. Cardell, D. A. Cremers, and J. J Laserna, Quim. Anal. (Barcelona) **18,** 169 (1999).
6. R. Barbini, F. Colao, R. Fantoni, A. Palucci, and F. Capitelli, Appl. Phys. A **69,** S175 (1999).
7. D. A. Cremers, M. H. Ebinger, D. D. Breshears, P. J. Unkefer, S. A. Kammerdiener, M. J. Ferris, K. M. Catlett, and J. R. Brown, J. Environ. Qual. **30,** 2202 (2001).
8. M. H. Ebinger, M. L. Norfleet, D. D. Breshears, D. A. Cremers, M. J. Ferris, P. J. Unkefer, M. S. Lamb, K. L. Goddard, and C. W. Meyer, Soil Sci. Soc. Am. J. **67,** 1616 (2003).
9. M. Martin, S. Wullschleger, and C. Garten, Proc. SPIE-Int. Soc. Opt. Eng. **4576,** 188 (2002).
10. M. Z. Martin, S. D. Wullschleger, C. T. Garten, Jr., and A. V. Palumbo, Appl. Opt. **42,** 2072 (2003).
11. G. A. Theriault, S. Bodensteiner, and S. H. Lieberman, Field Anal. Chem. Technol. **2,** 117 (1998).
12. P. A. Mosier-Boss, S. H. Lieberman, and G. A. Theriault, Environ. Sci. Technol. **36,** 3968 (2002).
13. A. K. Knight, N. L. Scherbarth, D. A. Cremers, and M. J. Ferris, Appl. Spectrosc. **54,** 331 (2000).
14. R. C. Wiens, R. E. Arvidson, D. A. Cremers, M. J. Ferris, J. D. Blacic, and F. P. Seelos, IV, J. Geophys. Res., Planets **107(No. E11),** 3–1 (2002).
15. R. Brennetot, J. L. Lacour, E. Vors, A. Rivoallan, D. Vailhen, and S. Maurice, Appl. Spectrosc. **57,** 744 (2003).
16. F. C. De Lucia, Jr., R. S. Harmon, K. L. McNesby, R. J. Winkel, Jr., and A. W. Miziolek, Appl. Opt. **42,** 6148 (2003).
17. A. Portnov, S. Rosenwaks, and I. Bar, J. Luminescence **102–103,** 408 (2003).
18. N. Reyniers, E. Vrindts, K. Dumont, J. De Baerdemaeker, and K. U. Leuven, Proc. SPIE-Int. Soc. Opt. Eng. **4542,** 36 (2002).
19. E. Vrindts, M. Reyniers, P. Darius, J. De Baerdemaeker, M. Gilot, Y. Sadaoui, M. Frankinet, B. Hanquet, and M.-F. Destain, Biosyst. Eng. **85,** 141 (2003).
20. R. J. Nordstrom, Appl. Spectrosc. **49,** 1490 (1995).
21. *Wavelengths and Transition Probabilities for Atoms and Atomic Ions Part II. Transition Probabilities, NSRDS-NBS 68* (U.S. Government Printing Office, Washington, D.C., 1980).
22. A. R. Striganov and N. S. Sventitskii, *Tables of Spectral Lines of Neutral and Ionized Atoms* (IFI/Plenum, New York, 1968).